



## *Acinetobacter baumannii* outer membrane protein A induces HeLa cell autophagy via MAPK/JNK signaling pathway



Zhiyuan An<sup>a,\*</sup>, Xiaoxi Huang<sup>a</sup>, Chunming Zheng<sup>a</sup>, Wenyi Ding<sup>b</sup>

<sup>a</sup> Medical Research Center, Beijing Chaoyang Hospital, Capital Medical University, Beijing 100020, China

<sup>b</sup> Department of Clinical Laboratory, Peking Union Medical College Hospital, Chinese Academy of Medical Sciences, Beijing 100730, China

### ARTICLE INFO

#### Keywords:

*Acinetobacter baumannii*  
Outer membrane protein A  
Autophagy  
HeLa cell line  
MAPK/JNK signaling pathway

### ABSTRACT

Autophagy is an evolutionary conserved self-balancing process that plays an important role in maintaining cellular homeostasis via the clearance of damaged organelles and misfolded proteins. Infection-triggered autophagy specifically inhibits the invasion of intracellular bacterial replication and hence protects the cells from microbial infections. It has been reported that *Acinetobacter baumannii* trigger cell autophagy. However, the role of its virulence protein OmpA remains unclear. Therefore, this study aimed to explore the effects of *Acinetobacter baumannii* OmpA on cell autophagy and its underlying molecular mechanisms. The results showed that OmpA induced autophagy in HeLa and RAW264.7 cells, increased LC3BII expression, and hindered p62 degradation. Moreover, OmpA triggered incomplete autophagy by interfering the fusion of autophagosomes with lysosomes. Besides, OmpA activated MAPK/JNK signaling pathway and enhanced the phosphorylation levels of JNK, p38, and ERK, c-Jun. Inhibition of JNK signaling pathway suppressed OmpA-induced autophagy in HeLa cells. Ab wild-type strains carrying OmpA triggered incomplete autophagy and resulted in a large number of IL-1 $\beta$  production. Ab- $\Delta$ OmpA strain (OmpA gene mutation) restored autophagic flux and reduced the accumulation of p62 and the release of IL-1 $\beta$  in HeLa cells. Rapamycin activated autophagy to inhibit OmpA-induced IL-1 $\beta$  secretion and protect HeLa cells from inflammatory damage. Collectively, these results suggest that OmpA can induce autophagy in HeLa cells through MAPK/JNK signaling pathway. Pre-treatment with Rapamycin activates autophagy and protects against cell death.

### 1. Introduction

*Acinetobacter baumannii* is a Gram-negative opportunistic pathogen that causes major infectious diseases such as pneumonia, septicemia and meningitis. The bacteria are commonly found among critically ill patients residing in the Intensive Care Unit. *Acinetobacter baumannii* has strong environmental stability and remains viable for a long period of time. In recent years, *Acinetobacter baumannii* has developed resistance to antibiotics as an inevitable consequence of antibiotic abuse, which confers a great challenge to disease treatment (Howard et al., 2012; Rice, 2008). In addition, *Acinetobacter baumannii* binds to the pattern recognition receptors and invades the host cells. Upon invasion, bacteria trigger the production of inflammatory cytokines and chemokines, leading to cell death via the disturbance of intracellular hemostasis (Lee et al., 2006; Bist et al., 2014).

Outer membrane protein A (OmpA) is the main virulence factor for *Acinetobacter baumannii*, which has always been closely related with the survival and pathogenicity of *Acinetobacter baumannii* (Sato et al., 2017;

McConnell et al., 2013; Jin et al., 2011). OmpA directly adheres and invades the host cells and thus leads to cell apoptosis through the destruction of nucleus and mitochondria (Choi et al., 2008a, b., Choi et al., 2005). Both *in vitro* and *in vivo* experiments have reported the decreased abilities of OmpA knockdown strains in replicating and adhering to host cells (Gaddy et al., 2009). If a patient is infected with *Acinetobacter baumannii* expressing high levels of OmpA, the toxic effects may be increased, leading to an increased risk of suffering pneumonia and bacteremia (Sánchez-Encinales et al., 2017).

The activation of autophagy requires multiple autophagy-related proteins to work together, such as LC3 and p62. LC3, namely microtubule-associated protein light chain 3 forms lipidated LC3II and is being recruited to autophagosomal membranes for autophagy activation (Mizushima et al., 2010; Glick et al., 2010). p62, also known as SQSTM1, is a ligand protein for LC3 binding, which is responsible for the degradation of ubiquitinated aggregates in autophagosomes. p62 can induce a complete autophagy after binding to LC3, and is excessively expressed upon the activation of autophagy. These key

\* Corresponding author at: Medical Research Center, Beijing Chaoyang Hospital, Capital Medical University, Beijing 100020, China.

E-mail address: [mran850712@aliyun.com](mailto:mran850712@aliyun.com) (Z. An).

autophagic proteins have been considered as useful markers for determining autophagic activity (Boyle and Randow, 2013; Evans et al., 2017).

Autophagy plays a key role in the host's innate immune response to bacteria (Kim et al., 2015; Dupont et al., 2009; Thurston et al., 2016). Autophagy regulates and eliminates many bacterial infections, including *Staphylococcus aureus*, *Shigella* and *Salmonella typhi*. However, the activation of autophagy may contribute to several undesirable side effects. For instance, *Brucella* activates and manipulates autophagy, by using energy substances in the autophagosomes to promote its survival and replication in host cells, and ultimately leads to cell death (Miller and Celli, 2016). Additionally, *Mycobacterium tuberculosis* utilizes the intracellular molecules to hinder the fusion of autophagosomes and lysosomes, in order to prevent degradation by autophagy (Sahu et al., 2017). Thus, it can be seen that bacteria have evolved a wide range of strategies to escape from autophagy. Besides, autophagy regulates the host inflammatory responses. For example, *Helicobacter pylori* CagA protein inhibits autophagy and results in an uncontrollable release of inflammatory cytokines (Li et al., 2017).

There are few studies reported on the autophagy induced by *Acinetobacter baumannii*, but the precise role of autophagy in inflammatory response remains largely unclear. It has been proposed that a virulence protein, Omp33-36, can induce the incomplete autophagy and assist the replication of *Acinetobacter baumannii* (Rumbo et al., 2014). Wang et al have reported that *Acinetobacter baumannii* induces the autophagy process via AMPK/ERK/mTOR signaling pathway, but what specific virulence proteins induced this process is not clear. (Wang et al., 2016). Recent studies have shown that *Acinetobacter baumannii* induces autophagy by activating the transcription factor EB. Moreover, it interferes with the autophagy-lysosomal system and destroys the lysosomal acidic environment to facilitate itself invasion and persistence (Parra-Millán et al., 2018). Other studies have suggested that *Acinetobacter baumannii* OmpA triggers cell apoptosis, but whether OmpA triggers autophagy and its underlying molecular mechanisms remain largely unclear. Therefore, this study aimed to explore the effects of *Acinetobacter baumannii* OmpA on cell autophagy and identify the molecular mechanisms underlying OmpA-induced autophagy.

## 2. Materials and method

### 2.1. Strains, reagents and antibodies

*Acinetobacter baumannii* ATCC 19606 (Ab-wild-type Ab-WT) was purchased from American Type Culture Collection (Manassas, VA, USA). *Acinetobacter baumannii* OmpA-mutant strains Ab- $\Delta$ OmpA was kindly provided by professor Jianrong SU. All bacterial strains were cultured in Luria-Bertani (LB) broth at 37 °C. *Escherichia coli* (E. coli) DH5a, E. coli BL21 (DE3), plasmid mini kit, gel recovery kit, high affinity Ni-NTA resin, and CCK8 reagent were purchased from Transgene Biotech (Beijing, China). pET21a (+) was purchased from Addgene. Restriction enzymes such as *XhoI* and *NdeI* were purchased from NEB. JNK inhibitors SP600125, 3-MA, Rapamycin, CQ were purchased from Sigma (Aldrich, St, Louis, MO, USA). LC3 A/B (12741), Beclin-1 (3495), JNK (9258S), p-JNK (4671S), p38 MAPK (9212), p-p38 MAPK (9211S), p-ERK (14474), ERK (12950), p-c-Jun (9164), Flag (14793), GAPDH (2118), His-Tag (12688) antibodies and JNK-siRNA (6232) / Control-siRNA (6568) were purchased from CST (Danvers, MA, USA). Antibodies p62 (ab56416) and IL-1 $\beta$  (ab9722) were purchased from Abcam (Cambridge, USA). Anti-rabbit or anti-mouse fluorescent secondary antibody was purchased from Zhongshan Golden Bridge Biological Company (Beijing, China). Lysotracker was purchased from Beyotimes Bio (Shanghai, China). Both mRFP-GFP-tfLC3 and GFP-LC3 plasmids were obtained from Hanheng Biotechnology Corporation (Wuhan, China). Lipofectamine 3000 was purchased from Invitrogen (Carlsbad, CA, USA). Apoptosis detection kit was purchased from Kaiji Biological Company (Nanjing, China). Primers and sequencing were

synthesized by AuGCT (Beijing, China).

### 2.2. Cell culture

Mouse macrophage cell line RAW264.7 (ATCC®TIB-71) and human cervical cancer cell line HeLa (ATCC®CCL-2) were obtained from American Type Culture Collection (ATCC). Fetal bovine serum and penicillin were purchased from Gibco (Grand Island, NY, USA). RAW264.7 cell line was cultured in DMEM complete medium containing 10% fetal bovine serum and 1% penicillin, whereas the HeLa cell line was cultured in RPMI 1640 complete medium containing 10% fetal bovine serum and 1% penicillin. Both cell lines were maintained at 37 °C in a humidified atmosphere of 5% CO<sub>2</sub>.

### 2.3. Expression and purification of *Acinetobacter baumannii* OmpA

The OmpA gene (GenBank: 485227) of *Acinetobacter baumannii* (ATCC 19606) containing *XhoI* and *NdeI* restriction sites was amplified by PCR. The PCR products were digested with *XhoI* and *NdeI* restriction enzymes prior to ligate with pET21a (+), in order to form an OmpA-pET21a (+) expression plasmid. After that, the expressed plasmid was transformed into E. coli BL21. The bacterial cells were collected by centrifugation, and then dissolved in binding buffer (1 M Tris, 150 mM NaCl, 0.1% TritonX-114, pH 8.0). The cells were sonicated in ice bath, followed by centrifugation at 12,000 rpm, 4 °C for 20 min. Subsequently, the supernatant was collected and purified by Ni-NTA affinity chromatography. Endotoxin in OmpA was removed by gel filtration chromatography (High-Capacity Endotoxin Removal Resin, Pierce, Thermo scientific). The samples were concentrated through ultrafiltration centrifugation (2000 MW cut off, Millipore) and stored at -80 °C. We further detected the LPS contamination in OmpA by using endotoxin quantitation kit (Endotoxin Detection Kit Limulus Amebocyte Lysate Kinetic Chromogenic Assay, Bioendo Technology Inc, Xiamen, China). The level of endotoxin in OmpA was less than 1 EU/ug. Thus, we suggested that the endotoxin in OmpA was very low, which was suitable for this study. Detection Identification of OmpA expression was performed using SDS-PAGE and Western blot. The membranes were incubated with His-tagged antibody overnight, and then with HRP-conjugated secondary antibodies for 1 h. Finally, the protein bands were visualized using ECL system (Amersham Pharmacia Biotech).

### 2.4. Morphological observation and cell viability of OmpA stimulated HeLa and RAW264.7 cells

The logarithmic growth phases of HeLa and RAW264.7 cells were seeded in 96-well culture plates at  $5 \times 10^3$  density in triplicate. DMEM or 1640 complete medium were added in each well, and then incubated at 37 °C, in a humidified atmosphere of 5% CO<sub>2</sub> for 24 h. After reaching 80% confluency, the cells were treated with different concentrations (0, 5, 10, 20, 40  $\mu$ g/mL) of OmpA or infected with Ab wild-type / Ab OmpA-mutant strains (MOI = 10:1) for 24 h. After incubation with 10  $\mu$ l CCK8 for 3 h at 37 °C, the OD of cells was read at 450 nm, by using a microplate reader (Tecan, Salzburg, Austria). The cell viability was calculated as: Cell viability = [OD (OmpA) - OD (blank)] / [OD (untreated) - OD (blank)]. RAW264.7 and HeLa cells were stimulated with 10  $\mu$ g/mL OmpA for 24 h, the morphologies of them were observed under an inverted microscope (Nikon, Tokyo, Japan).

### 2.5. Apoptotic rates of RAW264.7 and HeLa cells induced by OmpA

Apoptosis was detected using Annexin V-PI Apoptosis Assay kit (KeyGene BioTECH, Nanjing, China). HeLa and RAW264.7 cells were seeded in 6-well culture plates at  $5 \times 10^4$  density. After 24 h of incubation, both HeLa and RAW264.7 cell lines were stimulated with 10  $\mu$ g/ml OmpA for 24 h, followed by washing with PBS buffer for three

times. A total number of  $1 \times 10^5$  cells were collected and suspended in 500  $\mu$ l of binding buffer. Subsequently, 5  $\mu$ l of Annexin V and Propidium iodide (PI) were added and incubated for 15 min at room temperature in the dark. Lastly, the apoptosis rate was detected by FACS CantoII flow cytometry (Becton Dickinson, CA). Annexin V + and PI- were used to measure early apoptosis, while Annexin V + and PI + for late apoptosis. The sum of these two apoptotic rates was equal to the total rate of apoptosis. Graphical analysis was carried out using Flowjo (Treestar).

## 2.6. Autophagosomes detected by TEM

HeLa and RAW264.7 cells were seeded at  $5 \times 10^4$  density in 6-well culture plates. After 24 h of incubation, both HeLa and RAW264.7 cells were stimulated with 10  $\mu$ g/ml OmpA for 24 h. Then, the cells were centrifuged at 300 g for 5 min. The collected cell pellets were incubated with 2.5% glutaraldehyde at 4 °C for 2 h, and washed with PBS for three times. Subsequently, the cells were fixed with 1% osmium tetroxide at room temperature for 2 h, and washed three times with PBS. The cells were dehydrated and infiltrated with gradient ethanol of 50%, 70%, 80%, 90% for 10 min in each concentration. Agglutinated cells were embedded in epoxy resin, and cut into 70 nm thickness by using a microtome (Leica, Deerfield, IL). Finally, the cells were stained with uranyl acetate and lead nitrate. The prepared sections were subjected to high-resolution visualization under a transmission electron microscope (HT7700, Hitachi, Japan).

## 2.7. Western blotting analysis

HeLa cells and RAW264.7 cells were stimulated by OmpA for different time and concentrations or HeLa cells were infected with Ab wild-type / Ab OmpA mutant strains (MOI = 10:1) for different time. Then, these cells were collected and washed three times with PBS buffer. RIPA lysis solution was used to lyse the cells on ice for 20 min, followed by centrifugation at 12,000 g for 10 min to collect protein supernatants. BCA kit was used to determine the total protein concentration. Electrophoresis was performed on 10% or 15% SDS-PAGE gels, and transferred the proteins onto 0.22  $\mu$ m or 0.45  $\mu$ m PVDF membranes (Merck Milipore, Boston, USA). After blocking with 5% skimmed milk powder at 25 °C for 1 h, the target band was obtained and incubated overnight with the corresponding primary antibody at 4 °C. The membrane was washed three times for 10 min with TBST buffer, followed by the fluorescently-labeled goat anti-rabbit or goat anti-mouse antibody (diluted 1: 15,000) at room temperature for 1 h, the membrane was washed three times with TBST for 10 min. The detection of protein expression was carried out by Odyssey® CLx equipment (LI-COR Biosciences). Finally, the gray values were analyzed by Image J.

## 2.8. Immunofluorescence staining and transfection of GFP-LC3

The RAW264.7 cells stimulated with 10  $\mu$ g/ml OmpA for 24 h, then fixed with 4% paraformaldehyde for 15 min, permeabilized with 0.3% Triton-X100 for 10 min and blocked for 1 h with 3% BSA. Sequentially, LC3 A/B antibody (CST 12741) was added and incubated overnight at 4 °C. After washing three times with PBS for 5 min each, anti-rabbit secondary antibody (Zhongshan Golden Bridge, China) was added and incubated at room temperature for 1 h. Nuclei were stained with 1  $\mu$ g/ml DAPI. The expression of LC3 in RAW264.7 cells were observed under a confocal microscopy (TCS SP8, Leica, US). GFP-LC3 was transiently transfected into HeLa cells using lipofectamine 3000 (Invitrogen) according to the manufacturer's instructions. After transfection, the cells were stimulated with 10  $\mu$ g/ml OmpA or infected with Ab wild-type / Ab OmpA-mutant strains (MOI = 10:1) for 24 h. Finally, LC3 puncta were observed by using confocal microscopy. In some experiments, HeLa cells were pretreated with 5 mM 3-MA for 2 h or 5  $\mu$ M Rapamycin for 6 h before stimulated with 10  $\mu$ g/ml OmpA for 24 h. Fluorescence

microscopy (IX-51, Olympus, Japan) or confocal microscopy was used to detect the LC3 puncta.

## 2.9. LC3 turnover assay

LC3-turnover assay can identify whether the aggregated autophagosomes in cells are caused by the increase of autophagosomes or by the degradation barrier of autophagosomes. Lysosomal inhibitor CQ alters lysosomal pH and inhibits H<sup>+</sup> and ATPase, thereby preventing lysosomal acidosis for the inhibition of autophagosome degradation and the induction of incomplete autophagy (Klionsky et al., 2007). In the case of complete autophagy, the expression of LC3BII increased significantly after adding CQ. This observation indicates the normal process of autophagy degradation. In fact, the enhanced expression of LC3BII protein reflects the lysosomal degradation of autophagosomes (Ni et al., 2011). In our experiments, HeLa cells were pre-treated with 50  $\mu$ M CQ for 6 h and then stimulated with OmpA or Ab wild-type / Ab OmpA-mutant strains (MOI = 10:1) for 24 h. Western blot was used to detect the expression levels of LC3BII expression.

## 2.10. Detection of autophagy flux by mRFP-GFP-tfLC3 and lysotracker staining

Autophagic process is detected with mRFP (green fluorescent protein) tandem fluorescent-tagged LC3 (tfLC3) by using flow cytometry. GFP proteins are quenched in acidic autolysosomes, while mRFP proteins are expressed relatively stable in the acidic environment of autolysosomes. Only mRFP fluorescence is observed if the autophagic process appeared to be normal. However, a disturbance of autophagosomes and lysosomal fusion indicated that both GFP and mRFP fluorescence expressed yellow fluorescence, along with co-localization (Kimura et al., 2007). In our experiment, HeLa cells were seeded on 24-well plates and cultured for 24 h. The mRFP-GFP-tfLC3 reporter plasmid was transiently transfected into HeLa cells for 24 h by using lipofectamine 3000. The cells were then stimulated with OmpA alone or pre-treated with 5  $\mu$ M Rapamycin or 50  $\mu$ M CQ for 6 h, followed by co-incubation with 10  $\mu$ g/ml OmpA for 24 h. GFP-LC3 and mRFP-LC3 puncta were observed by confocal microscopy. In another experiment, HeLa cells transfected with GFP-LC3 for 24 h were treated with 10  $\mu$ g/ml OmpA for 24 h. The cells were then incubated with 50 nM LysoTracker red (Beyotime, China) for 30 min and washed three times with PBS for 5 min each step. Finally, the colocalization of GFP-LC3 with lysosome was observed under a fluorescent microscope.

## 2.11. RNA interference

Small interfering RNAs targeting JNK was purchased from CST (Danvers, MA, USA). HeLa cells were transfected with siRNAs by Lipofectamine RNAiMAX (Invitrogen, Carlsbad, CA, USA) according to the manufacturer's instructions. After 48 h of transfection, HeLa cells were stimulated by 10  $\mu$ g/ml OmpA for 24 h. Knockdown efficiency was determined by Western blot analysis. Three independent transfection experiments were performed.

## 2.12. Co-immunoprecipitation (Co-IP) analysis

HeLa cells were seeded in 100-mm dishes, when reaching 70% density, cells were transiently transfected with a total of 13  $\mu$ g of pcDNA3.1(+) or pcDNA3.1(+)-Flag-OmpA plasmids using Lipofectamine 3000 (Invitrogen). After 48 h of transfection, cells were harvested and lysed with NP40 lysis buffer (Beyotime, P0013F) for 30 min, followed by centrifugation at 12,000 rpm for 10 min to collect protein supernatants and then rotated with protein A + G Agarose (Santa Cruz) for 2 h at 4 °C to reduce nonspecific binding. After that, specific primary antibodies [anti-Flag (CST, Cat#14793) / anti-JNK (CST, Cat#9258S)] and the protein A + G Agarose were added in

supernatants, then incubated overnight at 4 °C with rotation. The beads-antibody-antigen complex was collected and washed three times with washing buffer. Then the beads was boiled at 100 °C for 10 min in 4 × SDS-PAGE loading buffer and analyzed by WB. Heavy chain interference in co-immunoprecipitation test was eliminated by IPKine™ HRP mouse anti-Rabbit IgG (Abbkine, Inc, China).

### 2.13. Enzyme-linked immunosorbent assay (ELISA)

HeLa cells ( $1 \times 10^6$  cells/well) were incubated with OmpA (10 µg/ml) for 24 h or infected with Ab wild-type and Ab OmpA-mutant strains (MOI = 10:1) for 6 h, 12 h, 18 h and 24 h. At the indicated times supernatant were collected and determined by ELISA with human IL-1β kit according to the manufacturer's instruction (R&D Systems, Minneapolis, MN). The absorbance of each well was detected by a microplate reader (Tecan, Salzburg, Austria).

### 2.14. Statistical analysis

All experimental data were expressed as mean ± SEM, and plotted with Prism 5.0 (GraphPad software Inc., San Diego, CA). Statistical analysis was performed using SPSS 17.0. Values of  $P < 0.05$  were considered statistically significant.

## 3. Results

### 3.1. Purification of *Acinetobacter baumannii* OmpA and its effects on HeLa and RAW264.7 cells apoptosis

High purity OmpA protein was obtained from Ni-column purification, and identified by SDS-PAGE and Western blot (Fig. 1A and B). To determine whether the purified OmpA was biologically active, we first observed the morphological and nucleus changes of HeLa and RAW264.7 cell lines after stimulating with 10 µg/ml OmpA for 24 h. The results demonstrated that both cell lines produced a wide range of cytoplasmic vacuolation, nucleus condensation and aggregation, as well as other apoptotic changes after the prolonged exposure to OmpA (Fig. 1C and D). Then, CCK8 assay was used to examine the inhibitory effect of OmpA on HeLa and RAW264.7 cells proliferation. The viability of HeLa and RAW264.7 cells were significantly inhibited by OmpA in a dose-dependent manner, with an IC50 of approximately 10 µg/ml (Fig. 1E). Next, OmpA-induced cell apoptosis was assessed by FITC Annexin V / PI flow cytometry. The results showed that RAW264.7 and HeLa cells were stimulated by 10 µg/ml of OmpA for 24 h could induce apoptosis, which was significantly higher than that of control group (Fig. 1F). Additionally, the phenomenon of OmpA-induced HeLa and RAW264.7 cell apoptosis was observed under transmission electron microscopy. Upon induction of 10 µg/ml OmpA, the morphological changes such as shrinkage, vacuolization of plasma membrane and mitochondria, as well as condensation of chromatin were observed in HeLa and RAW264.7 cells. (Fig. 1G). These results suggest that OmpA exhibit significant biological activities, including the inhibition of proliferation and induction of apoptosis in both HeLa and RAW264.7 cells.

### 3.2. *Acinetobacter baumannii* OmpA induces autophagy in HeLa and RAW264.7 cells

Many bacteria and their virulence factors can trigger the cell autophagy (McEwan, 2017; Bah and Vergne, 2017). In order to examine whether OmpA trigger autophagy in HeLa and RAW264.7 cells, the following experiments were conducted. First, we observed that the amount of LC3 puncta in cytoplasm of both cell lines were significantly increased after treating with 10 µg/ml OmpA for 24 h (Fig. 2A and 2B). Further, HeLa and RAW264.7 cells were initially treated with 0, 5, 10 µg/ml OmpA for 24 h or 10 µg/ml OmpA for 0 h, 12 h, 24 h, western

blotting was used to detect the expression of autophagy proteins LC3B and p62. The results demonstrated that the expression of LC3BII and p62 were increased in RAW264.7 and HeLa cells in a time- and dose-dependent manner (Fig. 2C to F). Besides, Transmission electron microscopy has been considered as the gold standard for autophagy detection, which can be used to examine the ultrastructure of autophagosomes in cells (Mizushima et al., 2010). We observed that OmpA triggered HeLa and RAW264.7 cells to produce a typical bilayer (onion-like) structure of autophagosomes, while both cell lines in the untreated group remained intact with healthy endoplasmic reticulum and mitochondria. Thus, these findings indicate that autophagy is induced by OmpA (Fig. 2G). To evaluate the autophagic capability of OmpA in HeLa cells, we established a GFP-OmpA transient HeLa cells line was established to assess the effect of OmpA overexpression on autophagy in HeLa cells. First, the expression of OmpA in HeLa cells was detected by Western blot, and the results confirmed that OmpA was successfully overexpressed in HeLa cells. Furthermore, OmpA overexpression significantly increased the expression levels of LC3BII, p62 and Beclin-1, which consistent with the results of p62 expression obtained from OmpA-stimulated HeLa cells (Fig. 2H). Collectively, these results suggest that OmpA can trigger autophagy in both HeLa and RAW264.7 cells, but may be limited to incomplete autophagy.

### 3.3. Interference of autophagosome and lysosomal fusion by *Acinetobacter baumannii* OmpA induces incomplete autophagy in HeLa cells

To further verify whether OmpA can trigger the incomplete autophagy, CQ was used to capture the process of autophagy. CQ is a drug that inhibits the fusion of autophagosomes and lysosomes, and induces the incomplete autophagy. There was no significant increase of LC3BII expression after the co-incubation of OmpA with 50 µM CQ, indicating that OmpA might induce incomplete autophagy in HeLa cells (Fig. 3A). LysoTracker staining revealed that GFP-LC3 was not co-localized with lysosomes, suggesting that autophagosomes were not fused with lysosomes (Fig. 3B). Detection of autophagy with mRFP-GFP-tfL3 showed that Rapamycin induced the complete autophagy in HeLa cells, by upregulating mRFP expression and downregulating GFP expression. Meanwhile, CQ could induce the simultaneous expression of mRFP and GFP fluorescence, through the colocalization of bright yellow fluorescence. However, the intensities of mRFP and GFP fluorescence in OmpA-stimulated group were similar to those in CQ-treated group, indicating that OmpA inhibited the fusion of autophagosome and lysosome (Fig. 3C). These results suggest that OmpA disrupts the autophagosome maturation of HeLa cells and interferes with the fusion of lysosomes, in order to trigger incomplete autophagy.

### 3.4. *Acinetobacter baumannii* OmpA induces HeLa cell autophagy via MAPK/JNK signaling pathway

MAPK signaling pathway involving p38, JNK and ERK plays an important role in cell proliferation and apoptosis, as well as autophagy (Dhillon et al., 2007; Zhou et al., 2015a,b). Western blotting was used to determine whether MAPK/JNK signaling pathway is associated with OmpA-induced HeLa cell autophagy. The results demonstrated that overexpression of OmpA in HeLa cells or stimulation of HeLa cells with OmpA could promote the phosphorylation levels of JNK, p38, ERK and c-Jun. (Fig. 4A and B). Subsequently, we co-treated HeLa cells with 10 µM of JNK-specific inhibitor SP600125 and 10 µg/ml OmpA for 24 h. Our findings revealed the phosphorylation levels of JNK, p38, ERK, c-Jun as well as the expression of LC3BII and Beclin-1 were decreased in co-treated group compared to OmpA alone group (Fig. 4C). Moreover, the viability of HeLa cells in co-treated group was significantly lower than OmpA alone group (Fig. 4D). To exclude the possibility that the autophagy inhibition by SP600125 was the result of a nonspecific drug, we examined the effect of siRNA-mediated JNK knockdown on OmpA-induced autophagy in HeLa cells. Western blotting showed that si-JNK

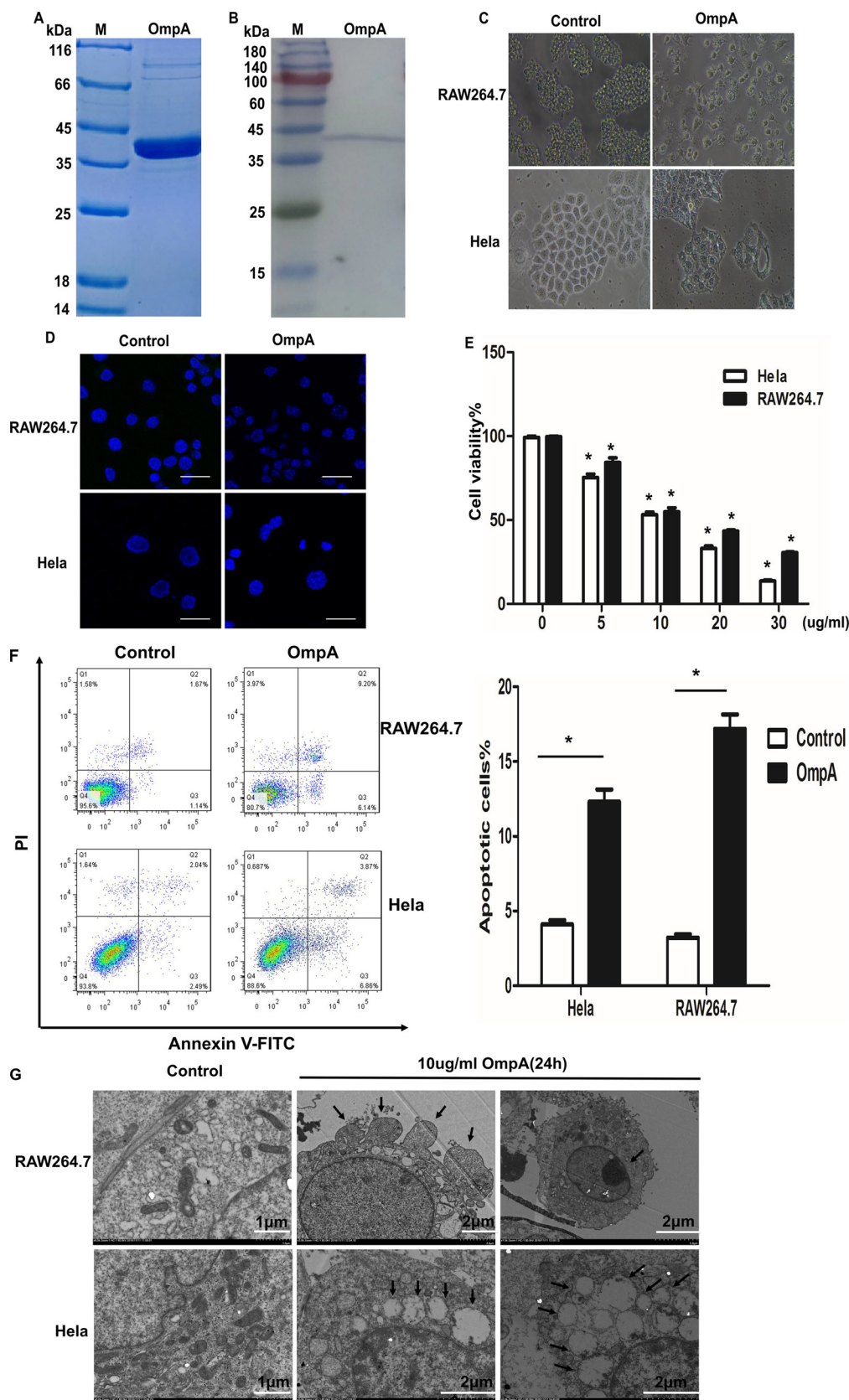


**Fig. 1.** Purification of OmpA of *Acinetobacter baumannii* and its leads to HeLa and RAW264.7 cells apoptosis. (A): Identification of OmpA expression by SDS-PAGE. (B): Identification of OmpA expression by Western blot. (C): The cell morphologic change of HeLa and RAW264.7 cells treated with 10  $\mu$ g/ml OmpA for 24 h (Magnification  $\times 20$ ). (D): DAPI staining showed that the nuclear morphological changes of HeLa and RAW264.7 cells with 10  $\mu$ g/ml OmpA for 24 h, Scale bar: 20  $\mu$ m. (E): The survival rate of HeLa and RAW264.7 cells treated with 0, 5, 10, 20, 40  $\mu$ g/ml OmpA for 24 h, which expressed as mean  $\pm$  SEM (n = 3), \*p < 0.05 vs control group. (F): The apoptosis rate of HeLa and RAW264.7 cells treated with 10  $\mu$ g/ml OmpA for 24 h, which detected by flow cytometry. The apoptosis rate was summarized as a histogram, \*p < 0.05 vs control group. (G): Detection of apoptosis induced by 10  $\mu$ g/ml OmpA stimulation for 24 h in HeLa and RAW264.7 cells by transmission electron microscopy.

significantly inhibited the total JNK and the phosphorylation levels of JNK and c-Jun. The expression of LC3B stimulated by OmpA was inhibited by si-JNK treatment, and the accumulation of p62 was also significantly reduced (Fig. 4E). We further identified the interaction

between OmpA and JNK by co-immunoprecipitation and immunofluorescence. As a result, we observed that p-JNK could enter into the nucleus after pcDNA3.1-flag-OmpA transfection into HeLa cells at 48 h by laser confocal microscopy. Meanwhile, we also found the co-

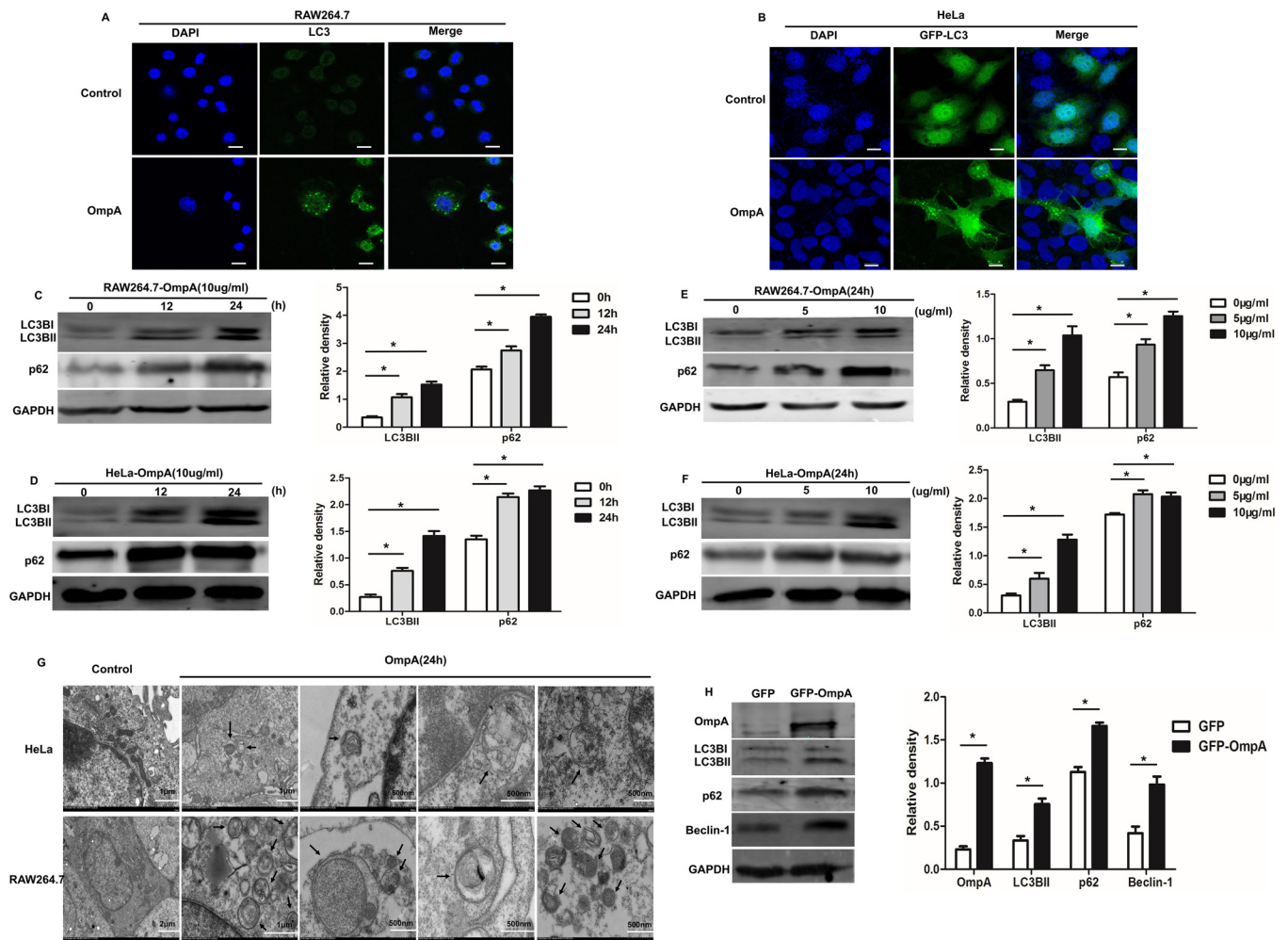


**Fig. 2.** *Acinetobacter baumannii* OmpA induces autophagy in HeLa and RAW264.7 cells. (A): Confocal microscopic detection of LC3 levels in 10 µg/ml OmpA stimulated or not stimulated RAW264.7 cells for 24 h, Scale bar: 10 µm. (B): Confocal microscopy was used to examine GFP-LC3 levels in 10 µg/ml OmpA stimulated or not stimulated HeLa cells for 24 h, Scale bar: 10 µm. (C–D): RAW264.7 and HeLa cells stimulated by 10 µg/ml OmpA for 0 h, 12 h and 24 h respectively. The expression levels of LC3B and p62 were detected by western blot. GAPDH was used as an internal control, \* $p < 0.05$  vs control group. (E–F): RAW264.7 and HeLa cells were stimulated with 0, 5, 10 µg/ml OmpA for 24 h. The expression levels of LC3B and p62 were detected by Western blot analysis. GAPDH was used as an internal control, \* $p < 0.05$  vs control group. (G): Transmission electron microscopy showed that 10 µg/ml OmpA stimulates HeLa and RAW264.7 cells for 24 h to induce autophagosome formation. The black arrows indicated typical autophagosomes. (H): Western blot was used to detect the expression levels of GFP-OmpA, LC3B, p62 and Beclin-1 in HeLa cells after transfection with GFP-OmpA plasmid for 48 h, GAPDH was used as an internal control, \* $p < 0.05$  vs control group.

localization of OmpA and endogenous JNK in cytoplasm and nuclear periphery (Fig. 4F–G). Similarly, co-immunoprecipitation results showed that OmpA could directly interact with JNK in HeLa cells (Fig. 4H). Based on these results, we believe that OmpA triggers an autophagy in HeLa cells via MAPK/JNK signaling pathway.

### 3.5. *Acinetobacter baumannii* OmpA is a key protein that cause incomplete autophagy in HeLa cells

In order to further confirm the effects of *Acinetobacter baumannii* OmpA on incomplete autophagy of HeLa cells, The HeLa cells were infected with Ab wild-type strain (Ab-WT) and Ab OmpA mutant strains (Ab- $\Delta$ OmpA) (MOI = 10:1) for different times, Western blot showed that the expression of LC3B in HeLa cells was significantly increased after infected with Ab-WT and Ab-OmpA. Next, We found that the level of p62 in HeLa cells infected with Ab-WT was significantly increased gradually with the time. Meanwhile, the level of p62 in Ab- $\Delta$ OmpA stimulation group was decreased in a time-dependent manner (Fig. 5A–B). Further, we infected HeLa cells with Ab-WT and Ab- $\Delta$ OmpA after treatment with lysosomal degradation inhibitor CQ, and then detected the expression of LC3B-II. As a result, the LC3B-II level

was no significant difference in Ab-WT infected group. But, turnover of LC3B-I to LC3B-II was increased in Ab- $\Delta$ OmpA infected group compared with Ab-WT infected group (Fig. 5C–D). In order to further demonstrate the role of OmpA on blocking the fusion of autophagosome and lysosomes, we transfected HeLa cells with GFP-LC3 and then infected with Ab-WT and Ab- $\Delta$ OmpA for 24 h. After that, we stained the LysoTracker red probe to trace lysosomes. Immunofluorescence results showed that GFP-LC3 could not co-localize with LysoTracker red in Ab-WT infected HeLa cells, which indicated that fusion of autophagosomes with lysosomes was interrupted. In contrast, GFP-LC3 colocalized with LysoTracker red in HeLa cells infected by Ab- $\Delta$ OmpA (yellow puncta), which proved that Ab- $\Delta$ OmpA led to the fusion of autophagosome and lysosome. Moreover, Fusion of autophagosomes and lysosomes enclosed by Ab-WT could be restored by Rapamycin. (Fig. 5E). Further, we detected the difference of IL-1 $\beta$  secretion and cell viability of HeLa cells between Ab-WT and Ab- $\Delta$ OmpA infected. The results showed that IL-1 $\beta$  secretion of HeLa cells was increased after infected with Ab-WT and Ab- $\Delta$ OmpA. Nevertheless, compared with the Ab-WT infected group, the secretion of IL-1 $\beta$  in the Ab-OmpA infected group was significantly reduced, thus improving the survival rate of HeLa cells. (Fig. 5F–G). Taken together, these results indicate that *Acinetobacter*

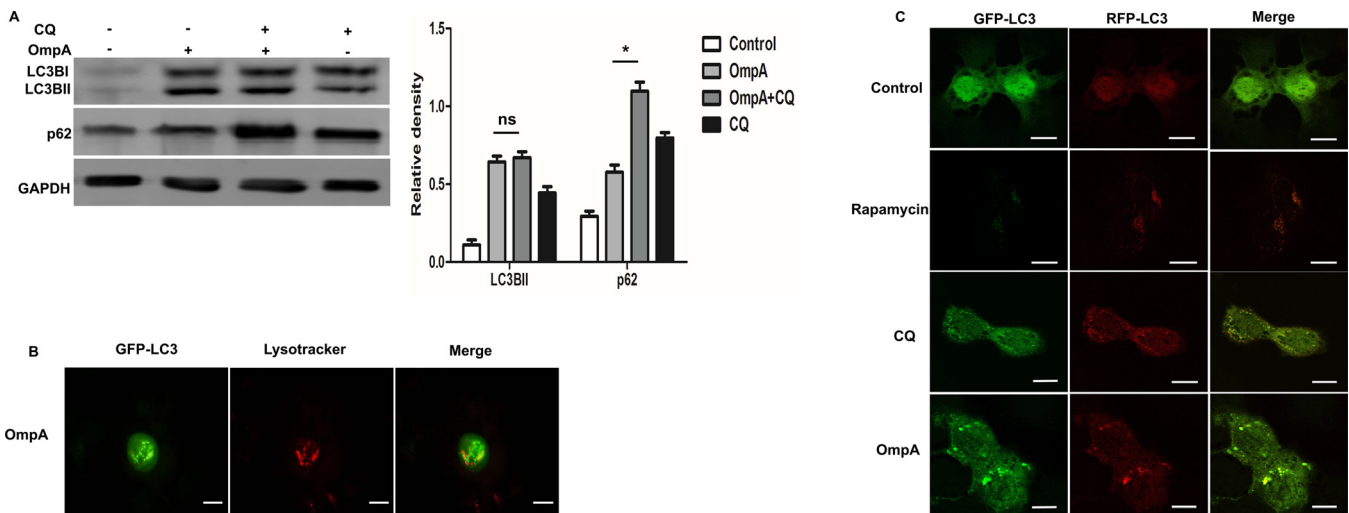


**Fig. 3.** *Acinetobacter baumannii* OmpA inhibits autophagy flux in HeLa cells (A): HeLa cells were pre-treated with 50  $\mu$ M CQ for 6 h and then induced by 10  $\mu$ g/ml OmpA for 24 h. The expressions of LC3 and p62 were detected by western blot. GAPDH was used as an internal control, \* $p < 0.05$  vs control group, ns: non-significant. (B): HeLa cells were transfected with GFP-LC3 plasmid for 24 h and then induced by 10  $\mu$ g/ml OmpA for 24 h. The co-localization of GFP-LC3 (green) and LysoTracker (red) was detected by fluorescence microscopy, Scale bar: 10  $\mu$ m. (C): mRFP-GFP-tfLC3 plasmids were transfected into HeLa cells for 24 h, pre-treated with 5  $\mu$ M Rapamycin or 50  $\mu$ M CQ for 6 h and then induced by 10  $\mu$ g/ml OmpA for 24 h. Confocal microscopy analysis of autophagy flux showed mRFP<sup>+</sup> GFP<sup>+</sup> as non-acidic autophagosomes, while mRFP<sup>+</sup> GFP<sup>-</sup> exhibited acidic autophagosome, Scale bar: 20  $\mu$ m (For interpretation of the references to colour in this figure legend, the reader is referred to the web version of this article).

*baumannii* OmpA is a key virulence protein that trigger incomplete autophagy in HeLa cells by inhibiting the fusion of autophagosome with lysosomes. In addition, Ab- $\Delta$ OmpA infect HeLa cells revert to complete autophagy, which is conducive to IL-1 $\beta$  clearance and improve cell viability.

### 3.6. The effects of 3 MA and Rapamycin on *Acinetobacter baumannii* OmpA induces IL-1 $\beta$ expression in HeLa Cells

The clearance of damaged organelles by autophagy is crucial for controlling excessive accumulation of inflammatory cytokines (Abdelaziz et al., 2015). We investigated whether the substitution of OmpA with 3-MA or Rapamycin can affect the activation of inflammatory cytokines in HeLa cells. 3-MA is a phosphatidylinositol 3 kinase (PI3K) kinase inhibitor that blocks the formation of autophagosome and inhibits autophagy. Rapamycin is an mTOR inhibitor that induces complete autophagy by increasing LC3BII expression and decreasing p62 expression (Mizushima et al., 2010). Our results showed that the cell viability was significantly decreased in 5 mM 3-MA and OmpA co-stimulation group compared to OmpA treatment group. On the contrary, cell viability was significantly increased in 5  $\mu$ M Rapamycin and OmpA co-stimulation group compared to OmpA treatment group. Moreover, Rapamycin treatment alone exhibited no significant effect on the proliferation of HeLa cells (Fig. 6A). In addition, Western blotting analysis revealed that the expression levels of LC3BII were significantly lower in 3-MA treatment and OmpA co-stimulation groups than those in OmpA-stimulation group. However, no significant change was observed for the expression level of p62. Furthermore, the expression level of IL-1 $\beta$  p17 was slightly increased compared to OmpA treatment group after autophagy inhibition (Fig. 6B). On the contrary, the expression levels of LC3BII were significantly higher in 5  $\mu$ M Rapamycin and OmpA co-stimulation group than those in OmpA treatment group. Concurrently, the expression levels of p62 and IL-1 $\beta$  p17 were significantly decreased. The results further indicated that Rapamycin could restore the autophagy flux and significantly decreased IL-1 $\beta$  p17 expression (Fig. 6C). Immunofluorescence staining revealed that the number of LC3 puncta were significantly lower in 3-MA and OmpA co-stimulation groups compared to OmpA treatment group. In contrast, the number of LC3 puncta were significantly increased in both

Rapamycin and OmpA co-stimulation group compared to OmpA treatment group, which was consistent with the results of Western blotting (Fig. 6D). In order to examine OmpA-induced IL-1 $\beta$  secretion, HeLa cells were treated with 10  $\mu$ g/ml OmpA for 24 h, then the secretion of IL-1 $\beta$  was detected by ELISA. The production of IL-1 $\beta$  was significantly increased by OmpA stimulation. Moreover, we found that Rapamycin could significantly inhibit the secretion of IL-1 $\beta$ , whereas 3-MA could significantly enhance the secretion of IL-1 $\beta$  (Fig. 6E). Taken together, we believe that autophagy of HeLa cells is inhibited by 3-MA, which enhances the inflammation reaction induced by OmpA and decreases the survival rate of HeLa cells. Rapamycin activates autophagy and reduces OmpA-mediated inflammation reaction, in order to protect against cellular damage in HeLa cells.

## 4. Discussion

This study confirmed that *Acinetobacter baumannii* OmpA induced apoptosis and autophagy in RAW264.7 and HeLa cells. However, OmpA increased p62 accumulation and interfered with the fusion of autophagosomes and lysosomes, leading to incomplete autophagy. Furthermore, The interaction between OmpA and JNK made the JNK phosphorylated and translocated into the nucleus. Inhibition of JNK signaling pathway significantly inhibited OmpA-mediated autophagy and decreased the expression of LC3B, Beclin-1 and accumulation of p62. Ab wild-type strains carrying OmpA triggered incomplete autophagy to enhance more production of the IL-1 $\beta$ . However, Ab- $\Delta$ OmpA strain (OmpA gene mutation) restored autophagic flux, thereby reducing the accumulation of p62 and the release of IL-1 $\beta$  in HeLa cells. Rapamycin activated autophagy of HeLa cells and inhibited OmpA-mediated IL-1 $\beta$  secretion and inflammatory damage. In sum, *Acinetobacter baumannii* OmpA causes incomplete autophagy and promotes the IL-1 $\beta$  release, which is regulated by JNK signaling pathway.

Many intracellular bacteria can trigger an autophagic response in host cells through autophagy, in order to eliminate other pathogens and maintain cellular homeostasis (Kimmy and Stallings, 2016). However, bacteria survived from autophagy may release specific the virulence factors to escape from autophagosome capture, by destroying autophagic vesicles and inhibiting ubiquitination. Otherwise, some bacteria can be protected from degradation, by interfering the fusion of

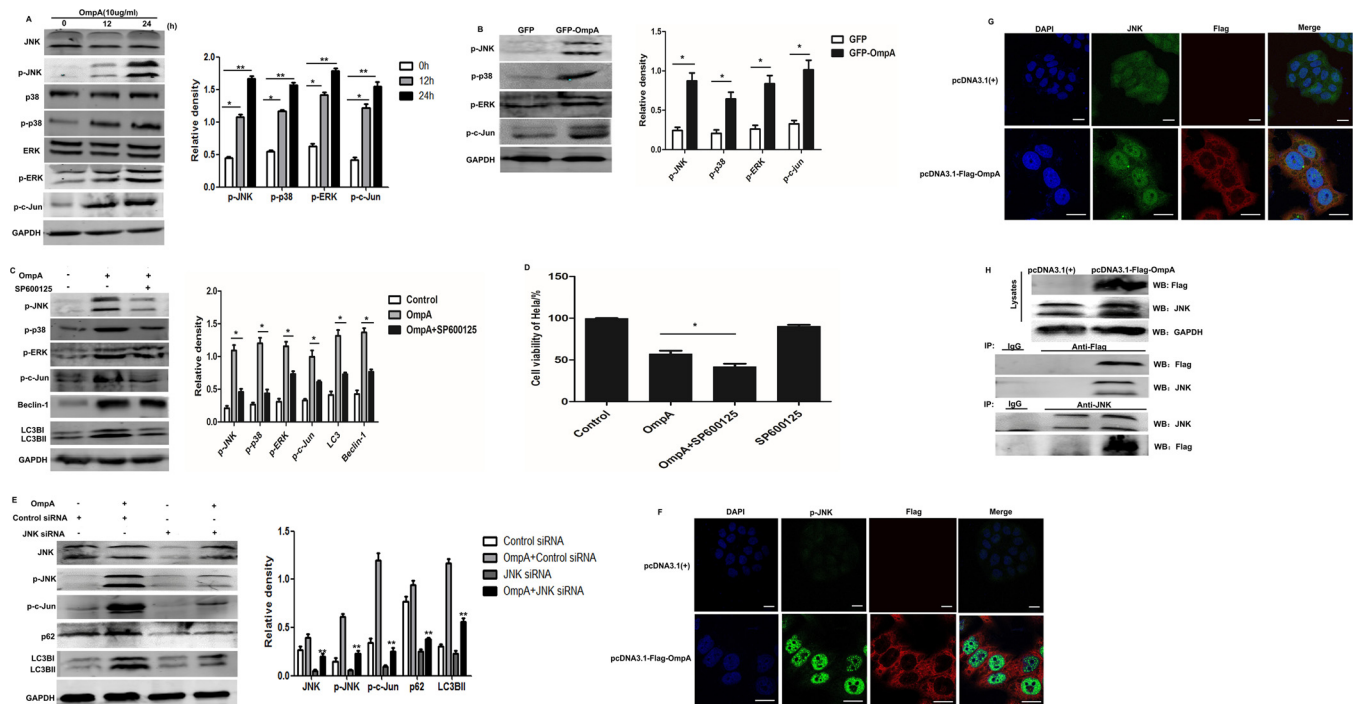


**Fig. 4.** *Acinetobacter baumannii* OmpA induces autophagy in HeLa cells via MAPK/JNK signaling pathway. (A): Western blot for the detection total of JNK, p38, ERK and JNK, p38, ERK, c-Jun phosphorylation levels in HeLa cells treated with 10  $\mu\text{g/ml}$  OmpA for 0 h, 12 h and 24 h. GAPDH was used as an internal control, \* $p < 0.05$ , \*\* $p < 0.01$  vs control group. (B): Western blot for the detection of JNK, p38, ERK and c-Jun phosphorylation levels after over-expression of OmpA in HeLa cells for 48 h. GAPDH was used as an internal control, \* $p < 0.05$  vs control group. (C): The expression of p-JNK, p-p38, p-ERK, p-c-Jun, LC3B and Beclin1 in HeLa cells co-treated with 10  $\mu\text{M}$  SP600125 and 10  $\mu\text{g/ml}$  OmpA, which detected by using Western blot. \* $p < 0.05$  vs OmpA group. (D): The inhibitory effect of SP600125 (10  $\mu\text{M}$ ) on HeLa cells, which was detected by CCK8. The results were expressed as mean  $\pm$  SEM ( $n = 3$ ), \* $p < 0.05$  vs OmpA group. (E): HeLa cells in which the expression of JNK was silenced using specific siRNA was transfected with siRNA-JNK or siRNA control for 48 h, then incubated with OmpA for 24 h, cell lysates were subjected to western blot analysis of JNK, p-JNK, p-c-Jun, LC3B and p62. The densitometry data are presented as the means  $\pm$  SEM of three independent experiments, \*\* $p < 0.01$  compared with OmpA + si Control group. (F): HeLa cells were transfected with pcDNA3.1-Flag-OmpA for 48 h and the expression of p-JNK was determined by Confocal microscopic. Confocal microscopic analysis indicated the OmpA triggered JNK phosphorylation as well as nucleus translocation in HeLa cells, Scale bar of empty vector group: 10  $\mu\text{m}$ , Scale bar of OmpA transfection group: 20  $\mu\text{m}$ . (G): Co-localization of OmpA with JNK. HeLa cells were transfected with pcDNA3.1(+) or pcDNA3.1-Flag-OmpA for 48 h. These cells were fixed and immune-stained with the anti-JNK as well as anti-Flag antibodies, labeled with anti-rabbit Alexa 488- (green) and anti-mouse Alexa 594- (red) fluorophore-conjugated secondary antibodies and imaged using confocal microscopy, Scale bar of empty vector group: 10  $\mu\text{m}$ , Scale bar of OmpA transfection group: 20  $\mu\text{m}$ . (H): HeLa cells were transfected with pcDNA3.1(+) or pcDNA3.1-Flag-OmpA for 48 h, both endogenous JNK fished by anti-Flag antibodies and exogenous Flag-OmpA fished by anti-JNK were detected using western blotting (For interpretation of the references to colour in this figure legend, the reader is referred to the web version of this article).

autophagosomes with lysosomal compartment (Miller and Celli, 2016). For instance, *Yersinia pestis* blocks the fusion of autophagosomes with lysosomes and promotes its replication in autophagic vesicles (Pujol et al., 2009). Besides, *Listeria monocytogenes* lyses autolysosome membranes via its virulence factor listeriolysin O LLO, allowing it to be released into the cytoplasm for proliferation and culminates in cell death (Vdovikova et al., 2017). Additionally, T3SS of *Salmonella typhi* inhibits the formation of autophagosome by activating mTOR (Owen et al., 2014). In the present study, we found that *Acinetobacter baumannii* OmpA induced the expression of LC3B in HeLa and RAW264.7 cells, in a time- and dose-dependent manner. However, as a ligand of LC3B, p62 expression was not correlated with LC3B expression. The expression of p62 did not decrease as the expression of LC3B increase. Furthermore, we confirmed that OmpA was able to inhibit autophagosome maturation, promoted incomplete autophagy.

Mitogen-activated protein kinase (MAPK) / JNK signal pathway plays a role in many basic cellular processes, such as proliferation, differentiation, stress response, apoptosis and survival (Arthur and Ley, 2013; Cargnello and Roux, 2011). As early as 2008, Kim reported that *Acinetobacter baumannii* OmpA can activate MAPK/JNK signaling pathway. However, the OmpA used in their study only activated p-JNK, p-ERK and p-p38 at 8 h, but with the prolongation of stimulation time (12 h, 24 h), the activation gradually weakened, and even had a significant inhibitory effect compared with the non-stimulation group. Our

study found that OmpA could continuously activate p-JNK, p-ERK, p-p38 and p-c-Jun within 24 h. We think that this discrepancy may be due to the different cell lines or experimental conditions used between the two studies. Recent studies have shown that MAPK/JNK signaling pathway regulates autophagy gene expression by activating downstream transcription factors c-Jun, c-Fos and FoxO. This signaling pathway plays an important role in autophagy regulation (Byun et al., 2009; Puissant et al., 2010; Zhou et al., 2015a,b). Our data showed that OmpA promoted p-JNK translocation into nucleus, which led to phosphorylation of transcription factors c-Jun to trigger autophagy. Inhibition of JNK signaling pathway significantly reduced the phosphorylation of JNK and c-Jun, and then inhibited the expression of LC3B and Beclin-1. More importantly, the accumulation of p62 was also degraded. We initially reveal the interaction between JNK and autophagy in *Acinetobacter baumannii* OmpA stimulated HeLa cells.

Although our research confirmed that both Ab-WT and Ab- $\Delta$ OmpA could cause autophagy in HeLa cells. But, Ab-WT blocked p62 degradation and prevented autophagosome and lysosome fusion, resulting in an incomplete autophagy. Nevertheless, Ab- $\Delta$ OmpA could restore autophagic maturation. These results suggest that OmpA plays a key role in the induction of incomplete autophagy, other virulence proteins may synergistically contribute to this process in *Acinetobacter baumannii* infection. In addition, Wang et al. have shown that *Acinetobacter baumannii* can induce a complete autophagy in HeLa cells. This is contrary

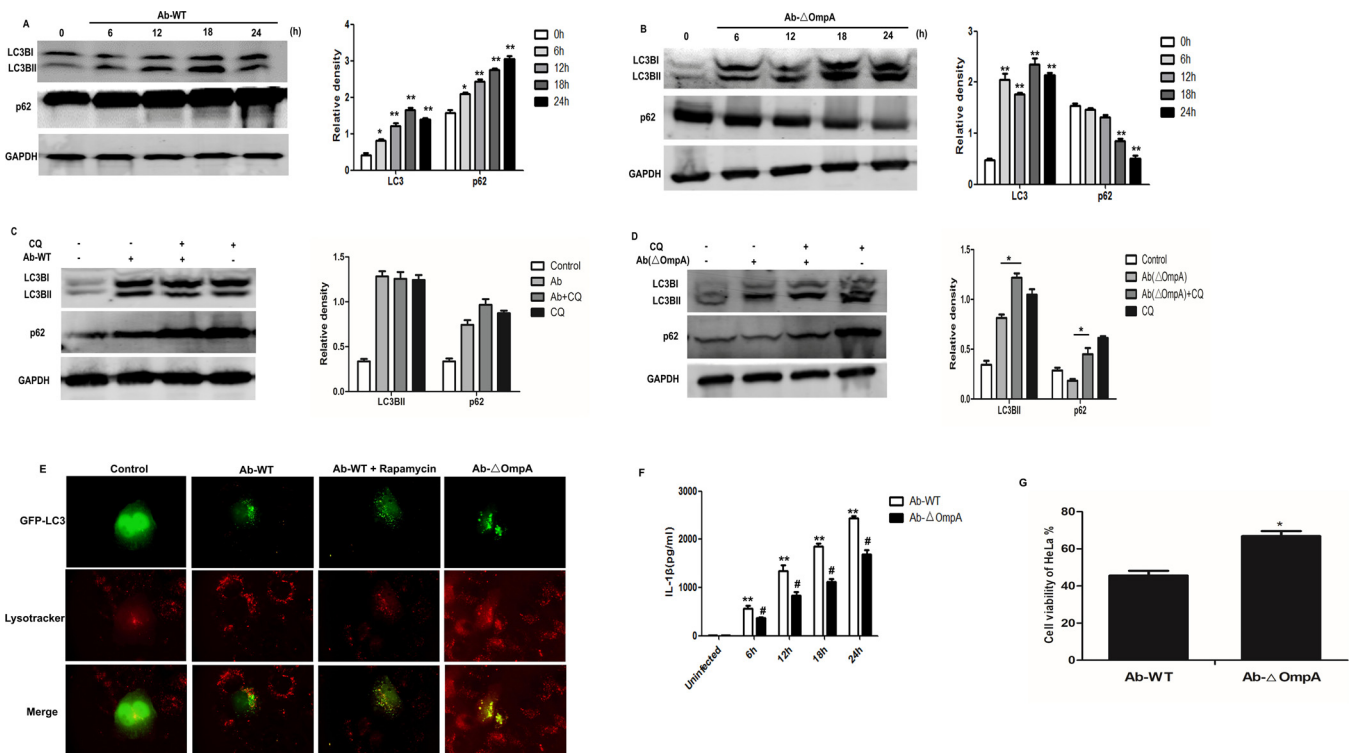


**Fig. 5.** *Acinetobacter baumannii* OmpA is a key protein that causes incomplete autophagy in HeLa cells (A): HeLa cells were infected with Ab wildtype strain (Ab-WT) for different times, The expression levels of LC3B and p62 were detected by Western blot analysis. GAPDH was used as an internal control, \* $p < 0.05$ , \*\* $p < 0.01$  vs control group. (B): HeLa cells were infected with Ab OmpA mutant strains (Ab- $\Delta$ OmpA) for different times, The expression levels of LC3B and p62 were detected by Western blot analysis. GAPDH was used as an internal control, \* $p < 0.05$ , \*\* $p < 0.01$  vs control group. (C): HeLa cells were pre-treated with 50  $\mu$ M CQ for 6 h and then infected with Ab-WT for 24 h. The expressions of LC3 and p62 were detected by western blot. GAPDH was used as an internal control, \* $p < 0.05$  vs Ab-WT infected group, ns: non-significant. (D): HeLa cells were pre-treated with 50  $\mu$ M CQ for 6 h and then infected with Ab- $\Delta$ OmpA for 24 h. The expressions of LC3 and p62 were detected by western blot. GAPDH was used as an internal control, \* $p < 0.05$  vs Ab- $\Delta$ OmpA infected group. (E): HeLa cells were transfected with GFP-LC3 plasmid for 24 h and then infected with Ab-WT or Ab- $\Delta$ OmpA (MOI = 10:1) for 24 h. The co-localization of GFP-LC3 (green) and LysoTracker (red) was detected by fluorescence microscopy (Magnification  $\times 100$ ). (F): HeLa cells were infected by Ab-WT and Ab- $\Delta$ OmpA for 6, 12, 18 and 24 h respectively. The levels of IL-1 $\beta$  in the culture supernatants were determined by ELISA. \*\* $p < 0.01$  compared with the control group. # $p < 0.05$  compared with the Ab-WT group. (G): HeLa cells were infected by Ab-WT and Ab- $\Delta$ OmpA for 24 h. The cell viability was detected by CCK8. The results were expressed as mean  $\pm$  SEM ( $n = 3$ ), \* $p < 0.05$  vs Ab-WT (For interpretation of the references to colour in this figure legend, the reader is referred to the web version of this article).

to our conclusion. We think the reason for this discrepancy may be due to the different strains used in the two studies. This difference suggests that different strains of *Acinetobacter baumannii* may have different ways in their physiological activities. Moreover, Wang's study only used *Acinetobacter baumannii* to stimulate HeLa cells for 3 h without further prolong the observation time and the p62 degradation in their experiments is not statistically different. Their conclusion that *Acinetobacter baumannii* causes complete autophagy in HeLa cells is somewhat far-fetched. This difference remains to be studied in the future.

Inflammatory cytokines released by host immune cells may play a protective role in the body's defense against bacterial infections, but excessive inflammation can exert an adverse effect on human health (Kim et al., 2015; Li et al., 2016). The secretion and release of inflammatory cytokines are regulated by autophagy, whereas autophagy inhibition weakens its control of inflammatory cytokine release, and thus leads to an uncontrollable systematic inflammatory response (Harris, 2011). This study demonstrated that the autophagy activity was interrupted by OmpA and induced by the massive release of inflammatory cytokine IL-1 $\beta$  p17. Moreover, *Acinetobacter baumannii* carrying OmpA (OmpA-positive strain) could inhibit autophagic flux, led to excessive IL-1 $\beta$  production and reduced cell viability. In contrast, Ab- $\Delta$ OmpA infection restored autophagy flux, the secretion of IL-1 $\beta$  was significantly degraded by autophagy, which helped host cells to limit and remove inflammatory factors, the cell survival rate was significantly improved. Therefore, we believe that the interference of OmpA on autophagic clearance is the key factor that causes the

accumulation of IL-1 $\beta$  and cell damage. These findings provide new evidence on how *Acinetobacter baumannii* activates the severe systemic inflammatory reaction.

The overexpression of autophagy proteins may contribute to the uncontrollable proliferation of bacteria and trigger more severe inflammatory reaction. Several essential proteins are involved in autophagic pathways and knockdown of these key autophagy proteins with siRNA can actually inhibit the autophagy formation. Likewise, the use of certain chemical drugs play important roles in controlling bacterial proliferation, inhibiting inflammatory response and promoting autophagy (Cadwell et al., 2016). For instance, Rapamycin stimulates autophagy, suppresses lung inflammation and reduces the symptoms of pneumonia in experimental mice (Abdulrahman et al., 2011). Rapamycin also blocks *Mycobacterium tuberculosis*-induced proliferation and differentiation into myofibroblasts, and thus inhibits the development of pulmonary fibrosis (Verma et al., 2016). In this study, we demonstrated that Rapamycin activated autophagy, protected against *Acinetobacter baumannii* OmpA-stimulated incomplete autophagy, down-regulated IL-1 $\beta$  p17 expression and reduced IL-1 $\beta$  release in HeLa cells. Taken altogether, these data suggest that Rapamycin may reverse incomplete autophagy caused by *Acinetobacter baumannii* OmpA, which is thus conducive to reducing OmpA-mediated cellular inflammation.

## 5. Conclusions

The findings of the present study indicated that *Acinetobacter*

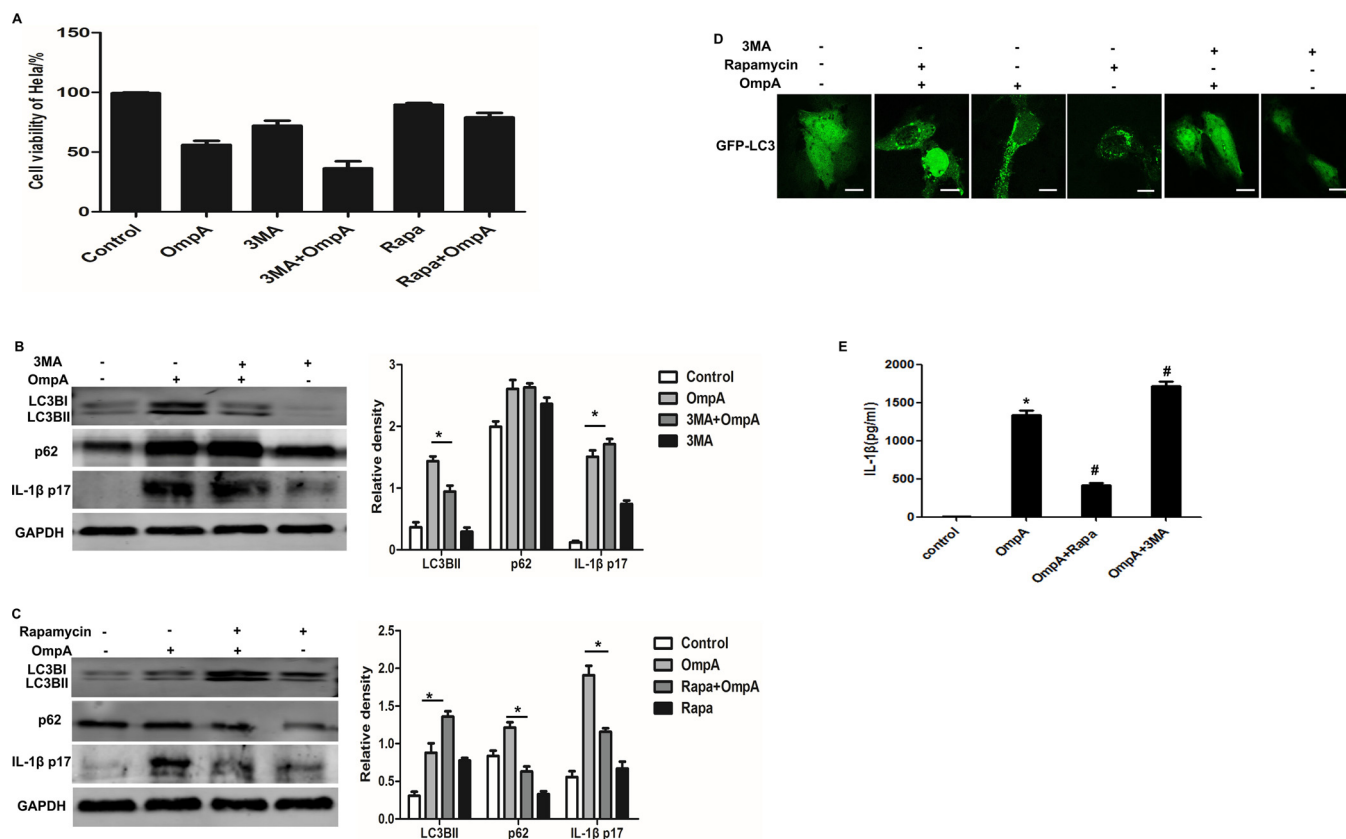


**Fig. 6.** The effects of 3MA and Rapamycin on *Acinetobacter baumannii* OmpA induces IL-1 $\beta$  expression in HeLa Cells (A): The inhibitory effect of 3-MA and Rapamycin on the proliferation of HeLa cells. The results were expressed as mean  $\pm$  SEM (n = 3), \*p < 0.05 vs OmpA group. (B): The HeLa cells were treated with 5 mM 3-MA for 2 h before co-stimulation with 10  $\mu$ g/ml OmpA for 24 h, Western blot was used to detect the expression levels of LC3B, p62 and IL-1 $\beta$  p17 in HeLa cells. GAPDH as internal control, \* p < 0.05 vs OmpA group. (C): After pre-treatment with Rapamycin at 5  $\mu$ M for 6 h before co-stimulation with 10  $\mu$ g/ml OmpA for 24 h, Western blot was used to detect the expression levels of LC3B, p62 and IL-1 $\beta$  p17 in HeLa cells. GAPDH was used as an internal control, \*p < 0.05 vs OmpA group. (D): GFP-LC3 plasmids were transfected into HeLa cells for 24 h, pre-treated with 5 mM 3-MA for 2 h or 5  $\mu$ M Rapamycin for 6 h, then co-stimulated with 10  $\mu$ g/ml OmpA for 24 h. Confocal microscopy was used to observe the expression levels of LC3. Scale bar: 10  $\mu$ m. (E): HeLa cells were pre-treated with 5 mM 3-MA for 2 h or 5  $\mu$ M Rapamycin for 6 h, then co-stimulated with 10  $\mu$ g/ml OmpA for 24 h. The levels of IL-1 $\beta$  in the culture supernatants were determined by ELISA. \*\*p < 0.01 compared with the control group. #p < 0.01 compared with the OmpA group.

*baumannii* OmpA blocked the fusion of autophagosomes and lysosomes, and interrupted the autophagy activity, resulting in an incomplete autophagy. Moreover, OmpA regulated autophagy through JNK signaling pathway. On the other hand, *Acinetobacter baumannii* OmpA mutant strains restored incomplete autophagy and decreased the production of IL-1 $\beta$ , improving cell survival rate. Autophagy activator Rapamycin inhibited OmpA mediated IL-1 $\beta$  production. This study provides a theoretical framework for understanding the pathogenic role of *Acinetobacter baumannii* OmpA in cell autophagy and inspiring new ways to treat infections.

#### Conflict of interest

The authors declare that they have no competing interests.

#### Funding

This work was supported by the National Natural Science Foundation of China (No. 81300049)

#### Acknowledgments

We acknowledge Dr. Jianrong SU (Clinical Laboratory center, Beijing Friendship Hospital, Capital Medical University, China) for providing us *Acinetobacter baumannii* OmpA mutant strains.

#### References

- Abdelaziz, D.H., Khalil, H., Cormet-Boyaka, E., Amer, A.O., 2015. The cooperation between the autophagy machinery and the inflammasome to implement an appropriate innate immune response: do they regulate each other? *Immunol. Rev.* 265, 194–204.
- Abdulrahman, B.A., Khweek, A.A., Akhter, A., Caution, K., Kotrange, S., Abdelaziz, D.H., Newland, C., Rosales-Reyes, R., Kopp, B., McCoy, K., Montione, R., Schlesinger, L.S., Gavrilin, M.A., Wewers, M.D., Valvano, M.A., Amer, A.O., 2011. Autophagy stimulation by rapamycin suppresses lung inflammation and infection by *Burkholderia cenocepacia* in a model of cystic fibrosis. *Autophagy* 7, 1359–1370.
- Arthur, J.S., Ley, S.C., 2013. Mitogen-activated protein kinases in innate immunity. *Nat. Rev. Immunol.* 13, 679–692.
- Bah, A., Vergne, I., 2017. Macrophage autophagy and bacterial infections. *Front. Immunol.* 8, 1483.
- Bist, P., Dikshit, N., Koh, T.H., Mortellaro, A., Tan, T.T., Sukumaran, B., 2014. The Nod1, Nod2, and Rip2 axis contributes to host immune defense against intracellular *Acinetobacter baumannii* infection. *Infect. Immun.* 82, 1112–1122.
- Boyle, K.B., Randow, F., 2013. The role of 'eat-me' signals and autophagy cargo receptors in innate immunity. *Curr. Opin. Microbiol.* 16, 339–348.
- Byun, J.Y., Yoon, C.H., An, S., Park, I.C., Kang, C.M., Kim, M.J., Lee, S.J., 2009. The Rac1/MKK7/JNK pathway signals upregulation of Atg5 and subsequent autophagic cell death in response to oncogenic Ras. *Carcinogenesis* 30, 1880–1888.
- Cadwell, K., 2016. Crosstalk between autophagy and inflammatory signalling pathways: balancing defence and homeostasis. *Nat. Rev. Immunol.* 16, 661–675.
- Cargnello, M., Roux, P.P., 2011. Activation and function of the MAPKs and their substrates, the MAPK-activated protein kinases. *Microbiol. Mol. Biol. Rev.* 75, 50–83.
- Choi, C.H., Lee, E.Y., Lee, Y.C., Park, T.I., Kim, H.J., Hyun, S.H., Kim, S.A., Lee, S.K., Lee, J.C., 2005. Outer membrane protein 38 of *Acinetobacter baumannii* localizes to the mitochondria and induces apoptosis of epithelial cells. *Cell. Microbiol.* 7, 1127–1138.
- Choi, C.H., Hyun, S.H., Lee, J.Y., Lee, J.S., Lee, Y.S., Kim, S.A., Chae, J.P., Yoo, S.M., Lee, J.C., 2008a. *Acinetobacter baumannii* outer membrane protein A targets the nucleus and induces cytotoxicity. *Cell. Microbiol.* 10, 309–319.
- Choi, C.H., Lee, J.S., Lee, Y.C., Park, T.I., Lee, J.C., 2008b. *Acinetobacter baumannii*

- invades epithelial cells and outer membrane protein A mediates interactions with epithelial cells. *BMC Microbiol.* 8, 216.
- Dhillon, A.S., Hagan, S., Rath, O., Kolch, W., 2007. MAP kinase signalling pathways in cancer. *Oncogene* 26, 3279–3290.
- Dupont, N., Lacas-Gervais, S., Bertout, J., Paz, I., Freche, B., Van Nhieu, G.T., van der Goot, F.G., Sansonetti, P.J., Lafont, F., 2009. *Shigella* phagocytic vacuolar membrane remnants participate in the cellular response to pathogen invasion and are regulated by autophagy. *Cell Host Microbe* 6, 137–149.
- Evans, T.D., Sergin, I., Zhang, X., Razani, B., 2017. Target acquired Selective autophagy in cardiometabolic disease. *Sci. Signal.* 10 pii: eaag2298.
- Gaddy, J.A., Tomaras, A.P., Actis, L.A., 2009. The *Acinetobacter baumannii* 19606 OmpA protein plays a role in biofilm formation on abiotic surfaces and in the interaction of this pathogen with eukaryotic cells. *Infect. Immun.* 77, 3150–3160.
- Glick, D., Barth, S., Macleod, K.F., 2010. Autophagy: cellular and molecular mechanisms. *J. Pathol.* 221, 3–12.
- Harris, J., 2011. Autophagy and Cytokines. *Cytokine* 56, 140–144.
- Howard, A., O'Donoghue, M., Feeney, A., Sleator, R.D., 2012. *Acinetobacter baumannii*: an emerging opportunistic pathogen. *Virulence* 3, 243–250.
- Jin, J.S., Kwon, S.O., Moon, D.C., Gurlung, M., Lee, J.H., Kim, S.I., Lee, J.C., 2011. *Acinetobacter baumannii* secretes cytotoxic outer membrane protein a via Outer Membrane Vesicles. *PLoS One* 6 e17027.
- Kim, J.Y., Paton, J.C., Briles, D.E., Rhee, D.K., Pyo, S., 2015. *Streptococcus pneumoniae* induces pyroptosis through the regulation of autophagy in murine microglia. *Oncotarget* 6, 44161–44178.
- Kimmy, J.M., Stallings, C.L., 2016. Bacterial Pathogens versus Autophagy Implications for Therapeutic Interventions. *Trends Mol. Med.* 22, 1060–1076.
- Kimura, S., Noda, T., Yoshimori, T., 2007. Dissection of the autophagosome maturation process by a novel reporter protein, tandem fluorescent-tagged LC3. *Autophagy* 3, 452–460.
- Klionsky, D.J., Cuervo, A.M., Seglen, P.O., 2007. Methods for monitoring autophagy from yeast to human. *Autophagy* 3, 181–206.
- Lee, J.C., Koerten, H., van den Broek, P., Beekhuizen, H., Wolterbeek, R., van den Barselaar, M., van der Reijden, T., van der Meer, J., van de Gevel, J., Dijkshoorn, L., 2006. Adherence of *Acinetobacter baumannii* strains to human bronchial epithelial cells. *Res. Microbiol.* 157, 360–366.
- Li, T., Xu, Y., Liu, L., Huang, M., Wang, Z., Tong, Z., Zhang, H., Guo, F., Chen, C., 2016. *Brucella melitensis* 16M regulates the effect of AIR domain on inflammatory factors, autophagy, and apoptosis in mouse macrophage through the ROS signaling pathway. *PLoS One* 11 e0167486.
- Li, N., Tang, B., Jia, Y.P., Zhu, P., Zhuang, Y., Fang, Y., Li, Q., Wang, K., Zhang, W.J., Guo, G., Wang, T.J., Feng, Y.J., Qiao, B., Mao, X.H., Zou, Q.M., 2017. *Helicobacter pylori* CagA protein negatively regulates autophagy and promotes inflammatory response via c-Met-PI3K/Akt-mTOR signaling pathway. *Front. Cell. Infect. Microbiol.* 7 doi: 10.3389.
- McConnell, M.J., Actis, L., Pachón, J., 2013. *Acinetobacter baumannii*: human infections, factors contributing to pathogenesis and animal models. *FEMS Microbiol. Rev.* 7, 130–155.
- McEwan, D.G., 2017. Host-pathogen interactions and subversion of autophagy. *Essays Biochem.* 61, 687–697.
- Miller, C., Celli, J., 2016. Avoidance and subversion of eukaryotic homeostatic autophagy mechanisms by bacterial pathogens. *J. Mol. Biol.* 428, 3387–3398.
- Mizushima, N., Yoshimori, T., Levine, B., 2010. Methods in mammalian autophagy research. *Cell* 140, 313–326.
- Ni, H.M., Bockus, A., Wozniak, A.L., Jones, K., Weinman, S., Yin, X.M., Ding, W.X., 2011. Dissecting the dynamic turnover of GFP-LC3 in the autolysosome. *Autophagy* 7, 188–204.
- Owen, K.A., Meyer, C.B., Bouton, A.H., Casanova, J.E., 2014. Activation of focal adhesion kinase by Salmonella suppresses autophagy via an Akt/mTOR signaling pathway and promotes bacterial survival in macrophages. *PLoS Pathog.* 10 e1004159.
- Parra-Millán, R., Guerrero-Gómez, D., Ayerbe-Algaba, R., Pachón-Ibáñez, M.E., Miranda-Vizuete, A., Pachón, J., Smani, Y., 2018. Intracellular trafficking and persistence of *Acinetobacter baumannii* requires transcription factor EB. *mSphere* 3 e00106-18.
- Puissant, A., Robert, G., Fenouille, N., Luciano, F., Cassuto, J.P., Raynaud, S., Auberger, P., 2010. Resveratrol promotes autophagic cell death in chronic myelogenous leukemia cells via JNK-mediated p62/SQSTM1 expression and AMPK activation. *Cancer Res.* 70, 1042–1052.
- Pujol, C., Klein, K.A., Romanov, G.A., Palmer, L.E., Citroa, C., Zhao, Z., Bliska, J.B., 2009. *Yersinia pestis* can reside in autophagosomes and avoid xenophagy in murine macrophages by preventing vacuole acidification. *Infect. Immun.* 77, 2251–2261.
- Rice, L.B., 2008. Federal funding for the study of antimicrobial resistance in nosocomial pathogens: no ESKAPE. *J. Infect. Dis.* 197, 1079–1081.
- Rumbo, C., Tomás, M., Fernández Moreira, E., Soares, N.C., Carvajal, M., Santillana, E., Beceiro, A., Romero, A., Bou, G., 2014. The *Acinetobacter baumannii* Omp33-36 porin is a virulence factor that induces apoptosis and modulates autophagy in human cells. *Infect. Immun.* 82, 4666–4680.
- Sahu, S.K., Kumar, M., Chakraborty, S., Banerjee, S.K., Kumar, R., Gupta, P., Jana, K., Gupta, U.D., Ghosh, Z., Kundu, M., Basu, J., 2017. MicroRNA 26a (miR-26a)/KLF4 and CREB-C/EBP $\beta$  regulate innate immune signaling, the polarization of macrophages and the trafficking of Mycobacterium tuberculosis to lysosomes during infection. *PLoS Pathog.* 13 e1006410.
- Sánchez-Encinales, V., Álvarez-Marín, R., Pachón-Ibáñez, M.E., Fernández-Cuenca, F., Pascual, A., Garnacho-Montero, J., Martínez-Martínez, L., Vila, J., Tomás, M.M., Cisneros, J.M., Bou, G., Rodríguez-Baño, J., Pachón, J., Smani, Y., 2017. Overproduction of outer membrane protein a by *Acinetobacter baumannii* as a risk factor for nosocomial pneumonia, bacteremia, and mortality rate increase. *J. Infect. Dis.* 215, 966–974.
- Sato, Y., Unno, Y., Kawakami, S., Ubagai, T., Ono, Y., 2017. Virulence characteristics of *Acinetobacter baumannii* clinical isolates vary with the expression levels of omps. *J. Med. Microbiol.* 66, 203–212.
- Thurston, T.L., Boyle, K.B., Allen, M., Ravenhill, B.J., Karpivovich, M., Bloor, S., Kaul, A., Noad, J., Foeglein, A., Matthews, S.A., Komander, D., Bycroft, M., Randow, F., 2016. Recruitment of TBK1 to cytosol-invading Salmonella induces WIPI2-dependent antibacterial autophagy. *EMBO J.* 35, 1779–1792.
- Vdovikova, S., Luhr, M., Szalai, P., Nygård Skalman, L., Francis, M.K., Lundmark, R., Engedal, N., Johansson, J., Wai, S.N., 2017. A novel role of *Listeria monocytogenes* membrane vesicles in inhibition of autophagy and cell death. *Front. Cell. Infect. Microbiol.* 7, 154.
- Verma, S.C., Agarwal, P., Krishnan, M.Y., 2016. Primary mouse lung fibroblasts help macrophages to tackle Mycobacterium tuberculosis more efficiently and differentiate into myofibroblasts up on bacterial stimulation. *Tuberculosis* 97, 172–180.
- Wang, Y., Zhang, K., Shi, X., Wang, C., Wang, F., Fan, J., Shen, F., Xu, J., Bao, W., Liu, M., Yu, L., 2016. Critical role of bacterial isochorismatase in the autophagic process induced by *Acinetobacter baumannii* in mammalian cells. *FASEB J.* 30, 3563–3577.
- Zhou, Yuan-Yuan, Li, Ying, Jiang, Wei-Qin, Zhou, Lin-Fu, 2015a. MAPK/JNK signalling: a potential autophagy regulation pathway. *Biosci. Rep.* 35 e00199.
- Zhou, Y.Y., Li, Y., Jiang, W.Q., Zhou, L.F., 2015b. MAPK/JNK signalling: a potential autophagy regulation pathway. *Biosci. Rep.* 35 pii: e00199.